Polymer Bulletin 22, 629–635 (1989)

Polymer Bulletin

The effects of hard segment content on microphase separation and physical properties of non-linear, segmented copolyureas formed by RIM

A.J. Birch, J.L. Stanford*, and A.J. Ryan**

Polymer Science and Technology Group, Manchester Materials Science Centre,
University of Manchester Institute of Science and Technology, Manchester M60 1QD, UK

Summary

The properties of RIM-copolyureas formed from a polyether triamine and containing 30 to 70% by weight of MDI/DETDA hard segments (HS) were investigated. As-moulded (mould temperature 115°C) and postcured (200°C/1h) materials were compared using DSC, DMTA and tensile stress-strain measurements. Phase separation ratios (PSR) of as-moulded materials increased from 47 to 56% with increasing HS content. Postcuring increased PSR to ~70% for all materials resulting in significant intensification of HS glass transition at Tg^H (220 to 250°C), and reduced mechanical damping and modulus-temperature dependence between -40 and 200°C. Agreement between experimental tensile moduli and those predicted by appropriate two-phase composite theory has confirmed the co-continuous morphology of these RIM-copolyureas over the entire composition range studied.

Introduction

The formation of copolyureas (1) from mixtures of aliphatic and aromatic amines reacting with aromatic isocyanates, occurs via competitive-consecutive reactions under the conditions prevalent in RIM. With branched reactants (2), a combination of chemical gelation, spinodal decomposition-induced microphase separation (3) and vitrification, as liquid is converted rapidly to solid, effectively quenches the system to yield a mixture of reaction products comprising homopolymers, various AB-type block copolymers and free monomers. This solid mixture possesses a non-equilibrium morphology (4,5) which arises from the direct competition between kinetics and thermodynamic changes occurring during the RIM process. It has been suggested (2,3,5,6) that such a morphology comprises co-continuous, soft- and hard-segment microphases, the coarseness of which may depend on hard-segment content. Further experimental evidence for these proposals is reported in this paper which directly supplements earlier work (2) by providing structure-property relations over a much wider composition range for non-linear copolyureas subjected to more intensive thermal annealing.

Experimental

Reactants

Copolyureas were formed from (a) a polyoxypropylene triamine, T5000 (ex. Texaco Chemicals), with a total amine equivalent weight of 1964±20 g mol^{-1}; (b) a hindered-diamine, 3,5-diethyl toluene diamine DETDA (ex. Lonza AG), an 80:20 mixture of 2,4- and 2,6-isomers; (c) a polyisocyanate, Isonate M340 (ex. Dow Chemical) based on 4,4' -methylenediphenylene diisocyanate (MDI), with an equivalent weight of 160.3±0.8 g mol^{-1}.

Reaction Injection Moulding and Materials Characterisation.

Rectangular plaques (240 x 150 x 3.5 mm) of the copolyureas were moulded using smaller-capacity RIM equipment (5) to that used in previous studies (2,7). (The use of slightly dissimilar RIM equipment, in terms of mix-head geometry, reactant throughputs and mould size, may result in small variations in structure and physical properties of materials with otherwise identical composition). The processing conditions used in the present study

*Author to whom correspondence should be addressed

**Present address: Department of Chemical Engineering and Materials Science, University of Minnesota, Minneapolis, MN 55455, USA

are summarised in Table 1. Hard segment content, defined as the mass of DETDA plus the stoichiometric equivalent mass of M340, divided by the total mass of the formulation, was varied from 30 to 70% by weight. RIM-materials were coded as UD with U referring to urea and D to DETDA, followed by a number representing the weight percentage hard segment content: letters NPC and HPC refer to non-postcured and high-temperature postcured.

Table 1. RIM-Processing Conditions used to form Copolyureas.

Initial reactant temperature	40°C
Mould temperature	115°C
Polyamine/diamine throughput	120 g s^{-1}
Polyamine/diamine Reynolds number (5)	> 330
Reactant stoichiometric ratio	1.03
High-temperature postcure schedule	200°C/1h

Characterisation of RIM-Copolyureas involved differential scanning calorimetry, DSC (using ~14 mg samples), dynamic mechanical-thermal analysis, DMTA, and tensile stress-strain measurements. Experimental details were identical to those previously reported(2).

Results and Discussion

The trifunctional, macro-network structure of the segmented copolyureas is represented schematically in figure 1. This ideal $(AB)_n$-type block copolymer nature of the RIM-materials, however, is only achieved at complete reaction (8). In the initial stages of copolymerisation, -NCO-tipped, polyether-urea oligomers are formed by the preferential reaction between aliphatic $-NH_2$ groups and the effectively large stoichiometric excess of -NCO groups, which also delays gelation. Essentially, the reactivity of the polyether soft-segment is reduced to approximately that of unreacted MDI so that subsequent DETDA/MDI hard segment development and copolyurea network formation then proceed more or less simultaneously. In this way, good connectivity between hard- and soft-segment is achieved, and rapid phase separation and hard segment vitrification thermodynamically quench the system producing a material with non-equilibrium, co-continous morphology.

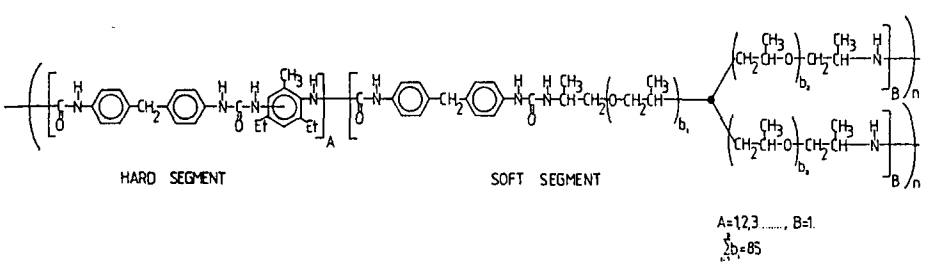

Figure 1. Idealised $(AB)_n$ block structure of segmented RIM-copolyureas.

Differential Scanning Calorimetry, DSC.

DSC data summarised in Table 2 were derived from at least 5 traces for each material. All traces showed only endothermic shifts around -60°C, extending over a temperature range of ~30°C, which result from the soft-segment glass transition. The temperatures corresponding to the onset of the base-line shifts were recorded to give values for Tg^S which are in reasonable agreement with those reported previously (2). The percentage degree of phase separation, PSR(%), was calculated for each material using the specific heat change ($\Delta Cp/m$) method at Tg^S (9). The PSR values in Table 2 are plotted in figure 2, together with previous data (2), and show quite clearly the effects of thermal annealing. The amount by which PSR increases on postcuring depends on hard segment content and cure temperature (and time).

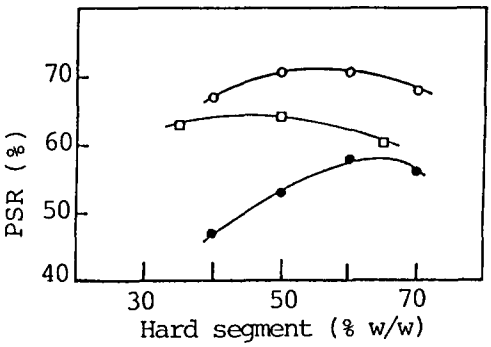

Table 2. The Effects of HS and Postcuring on Tg^S and PSR of RIM-Copolyureas.

Copoly-urea	Non-postcured Tg(°C)	PSR(%)	Postcured Tg(°C)	PSR(%)
UD30	-61	-	-61	-
UD40	-61	47	-60	67
UD50	-61	53	-60	71
UD60	-60	58	-59	71
UD70	-60	56	-59	68

T5000: Tg = -64°C (2)

Figure 2. The variation of PSR with HS content for RIM-copolyureas -●- NPC; -o- PC 200°C/1h; -□- PC 100°C/18h (previous data (2)).

The non-postcured copolyureas show a marked dependence of PSR on HS content: as HS content increases, the reaction exotherm during RIM also increases, delaying vitrification and therefore allowing greater (micro)phase separation to occur. Postcuring increases PSR by an amount which is dependent more on temperature than time, and at the higher postcure temperature of 200°C (top curve in figure 2), the value of PSR is essentially independent of HS content. The DSC data therefore suggests that postcuring allows these RIM-copolyureas to attain morphologies closer to equilibrium by diffusion-controlled processes which are described in the next section.

Dynamic Mechanical Thermal Analysis (DMTA).

The (micro)phase separated structure of the RIM-copolyureas, characterised by DSC, is confirmed by the DMTA data shown in figures 3 and 4. The essential dynamic properties derived from medial DMTA curves are summarised in Table 3.

Soft-segment and hard-segment glass transitions are clearly evident in figure 3 as tan δ peaks at temperatures Tg^S (~ -40°C) and Tg^H (220 to 250°C), and the peak intensities decrease and increase, respectively, with increasing HS content. Flexural modulus for each copolyurea in figure 4 shows the expected rapid decreases associated with the transitions at Tg^S and Tg^H, and the modulus-temperature dependence of the materials over the range -30 to 165°C is given by the modulus ratios in Table 3. The value of E'(-30°C) / E'(65°C) is

Table 3. Glass Transition Temperatures and Flexural Modulus Ratios of RIM-Copolyureas: Effects of Postcuring and Hard Segment Content.

Copolyurea	Tg^S		Tg^H		E'(-30°C)	E'(65°C)
	°C	tan δ	°C	tan δ	E'(65°C)	E'(160°C)
UD30NPC	-41	0.20	220(a)	0.30	10.4	1.7
UD30HPC	-40	0.20	220(a)	0.38	6.7	1.6
UD40NPC	-40	0.15	235	0.33	5.0	1.8
UD40HPC	-40	0.15	236	0.43	3.7	1.5
UD50NPC	-39	0.11	219	0.40	3.8	1.5
UD50HPC	-39	0.11	233	0.42	3.5	1.4
UD60NPC	-34	0.09	237	0.48	3.3	1.5
UD60HPC	-39	0.09	235	0.51	2.5	1.4
UD70NPC	-36	0.05	248	0.57	2.1	1.5
UD70HPC	-40	0.07	247	0.61	1.9	1.3

(a) Observed only as a shoulder in tan δ /temperature curves.

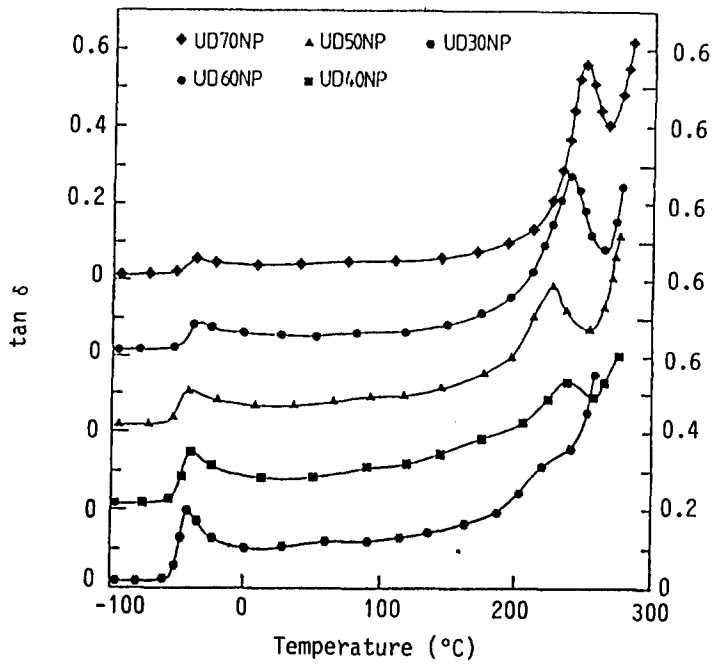

Figure 3. Damping versus temperature for RIM-copolyureas containing increasing HS content. (Curves shifted by 0.2 in tan δ.)

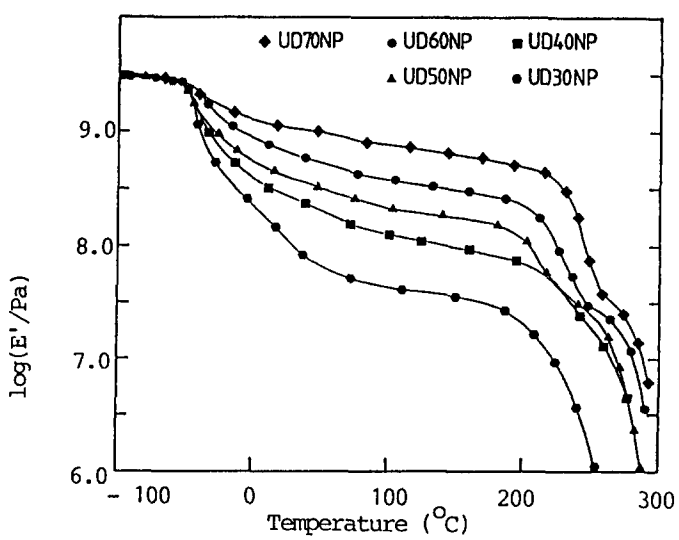

Figure 4. Storage modulus versus temperature for RIM-copolyureas containing increasing HS content.

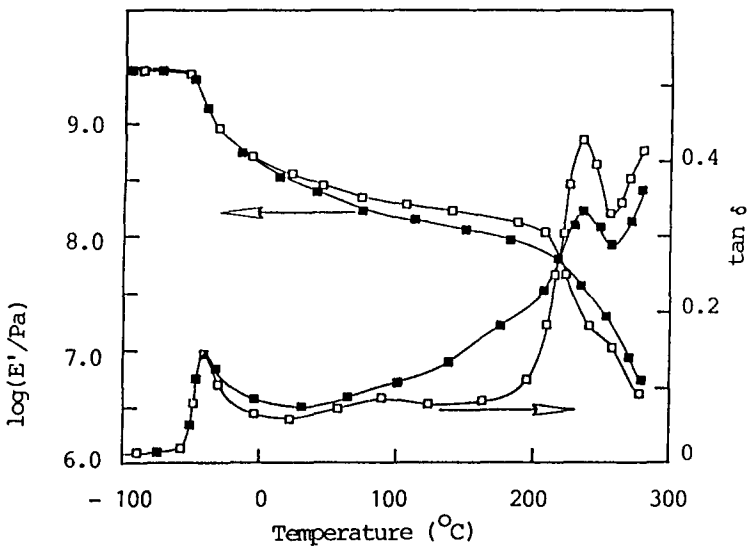

Figure 5. Storage modulus and damping versus temperature for 40% HS RIM-copolyureas; -■-, nonpostcured; -□- postcured.

dominated by the modulus at -30°C which is in the rapidly changing region around Tg^S: the ratio, therefore, shows a strong dependence on HS content. The higher temperature ratios, E'(65°C) / E'(160°C), show a small decrease with increasing HS content and the values, 1.3 to 1.8 compared to unity for the ideal material, reflect the very low temperature dependence of these RIM-copolyureas over a wide temperature interval extending up to 200°C.

In a previous publication (2), postcuring at 100°C/18h was shown to have only a small effect on the thermal-mechanical behaviour of similar RIM-copolyureas. In the present study, more severe postcuring conditions of 200°C/1h were used and as figure 5 shows, the effects on thermal-mechanical behaviour are significant particularly at higher temperatures. In general, postcuring increases flexural modulus and reduces the overall level of damping between -40 and 200°C. The steadily rising tan δ curve between 20 and 200°C is resolved into a weak but broad transition around 90°C and a more clearly defined glass transition at Tg^H. The former transition ranging from 50 to 120°C is attributed to the breakdown of phase-mixed structures in these RIM-copolyureas. In the materials with low HS contents, postcuring has negligible effects on the location and intensity of the soft segment transition, although its breadth is reduced. There is, however, a small but discernible downward shift in Tg^S at higher HS content (5) indicating the presence of purer soft-segment phases after postcuring. The biggest effect of postcuring is the intensification of the Tg^H transition (0.33 to 0.43 in tan δ) but without shifting its location.

These changes in thermal-mechanical behaviour on postcuring result mainly from the sharpening of domain boundaries between soft- and hard-segment (micro)phases which occurs by a diffusion process involving molecular flux of each type of segment against its concentration gradient. This process, called uphill diffusion (3), is facilitated by thermal annealing and promotes greater microphase separation, as indicated by the PSR values in Table 2. The overall effect, therefore, is to reduce the temperature dependence of the modulus at each composition, as shown by the modulus ratios in Table 3.

Tensile Stress-Strain Properties.

The wide range of materials behaviour, from soft elastomeric to rigid plastic, is illustrated by the averaged stress-strain curves in figure 6 and the derived tensile properties in Table 4. (The anomalously poor ultimate properties of UD30 are due to the presence of

Table 4. Tensile Properties of RIM-Copolyureas: Effects of HS Content and Postcuring.

	Non-postcured				Postcured			
	E (MPa)	σ_u (MPa)	ε_u (%)	U_t (MJ m^{-3})	E (MPa)	σ_u (MPa)	ε_u (%)	U_t (MJ m^{-3})
UD30	141	9.0	95	6.4	153	11.9	134	13.2
UD40	281	19.0	221	24.8	299	21.0	220	23.0
UD50	560	29.0	114	24.9	565	30.3	98	20.4
UD60	898	29.1	20	5.0	919	36.2	33	10.2
UD70	1352	30.7	4	0.6	1367	45.6	19	6.9

extensive flaws within the material formed by premature gel-line formation (4, 5) during mould filling.) In general modulus (E) and tensile strength (σ_u) increase with HS content, with concomitant decreases in elongation (ε_u) and tensile toughness (U_t). The improvements in tensile properties on postcuring are most apparent at higher hard segment contents with UD70, for example, showing an order of magnitude increase in materials toughness.

The variation of properties with HS content provides a useful insight into the type of morphological structure prevalent in RIM-copolymers. Figure 7(a) shows plots of modulus versus composition for the present copolyureas and for the chemically analogous RIM-copoly(urethane-urea)s (11). In the former, E changes with HS in a continuous manner, rising gradually with increasing HS up to 40% then showing a rapid, almost linear increase between 40and 70% HS. In contrast, the RIM-copoly(urethane-urea)s, formed from a polyether triol of similar Mn to T5000 and identical DETDA and polyisocyanate reactants, show lower overall values of modulus and a discontinuity at ~55% HS. The effects of changing soft segment functional groups from $-NH_2$ to -OH and the need to use high levels of catalysts with the latter (11) cause significant differences in polymerisation route, kinetics and (micro)phase separation during heterogeneous macro-network formation (6). Consequently, subtle differences in morphology and physical proprties arise in the finally-

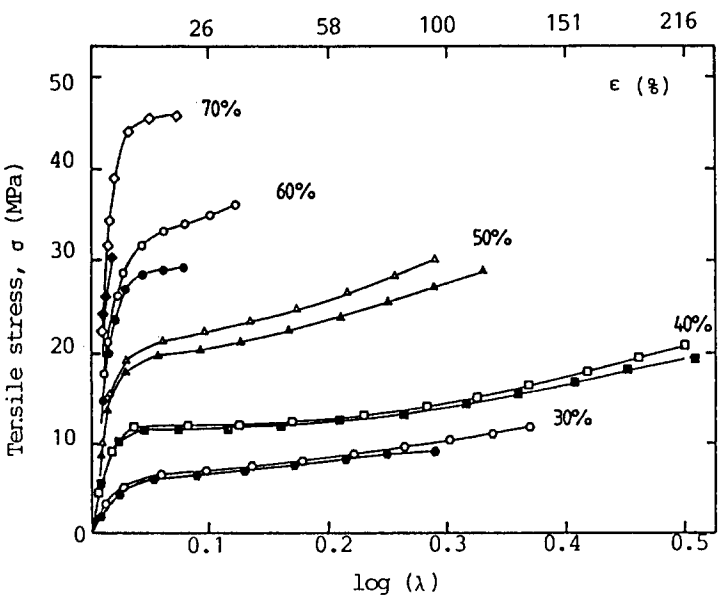

Figure 6. Tensile stress-strain curves for postcured (open symbols) and non-postcured (closed symbols) RIM-copolyureas containing 30-70% HS. λ is the extension ratio and ε the corresponding strain.

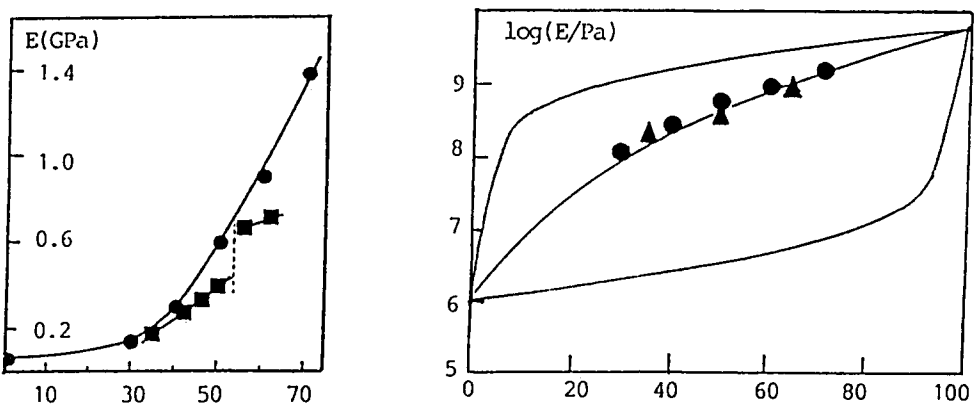

Figure 7. Tensile modulus versus HS content. (a) copolyureas -●- (present work) and copoly(urethane-urea)s -■- (previous work (11)); (b) copolyureas -●- (present work) , -▲- (previous work (2)) with curves predicted (6) by theory (12, 13).

formed, RIM-materials. Nevertheless, the data in figure 7(a) for both types of RIM-copolymers can be approximated to a simplified composite model (12) which assumes perfect bonding between two co-continuous phases.

Moduli predicted (6) using the co-continuous model are shown in figure 7(b) by the middle curve, in comparison with experimental moduli for the copolyureas of the present work (circles) and for those (triangles) reported previously (2). Also shown in figure 7(b) are upper and lower boundary curves for continuous-discontinuous, composite models (13) comprising, respectively, glassy matrix-rubbery spheres and rubbery matrix-glassy spheres. The excellent agreement between theory (12) and experiment over the wide range of copolymer composition studied therefore confirms the co-continuous morphology of these RIM-copolyureas.

Acknowledgement

The authors would like to thank the Texaco Chemical Company, Dow Chemical and Lonza AG for kindly supplying the chemical reactants used in this study.

References

1. Ryan, A.J., Stanford, J.L., in "Comprehensive Polymer Science", ed. by G. Allen and J.C. Bevington, Pergamon Press, Oxford, Ch. 25, **5**, 427 (1988).
2. Ryan, A.J., Stanford, J.L., Wilkinson, A.N., Polym. Bull. **18**, 517 (1988).
3. Ryan, A.J., Polymer *in press* (1989).
4. Willkomm, W.R., Chen, Z.S., Macosko, C.W., Gobran, D.H., Thomas, E.L., Polym. Eng. Sci. **28**, 888 (1988).
5. Stanford, J.L., Wilkinson, A.N., Lee, D-K., Ryan, A.J., Plast. Rubb. Proc. Appl. *in press* (1989).
6. Ryan, A.J., Stanford, J.L., Still, R.H., Plast. Rubb. Proc. Appl. *in press* (1989).
7. Barksby, N., Dunn, D., Kaye, A., Stanford, J.L., Stepto, R.F.T., in "Reaction Injection Molding", ed. by J.E. Kresta, ACS Symp. Ser. **270**, ACS, Washington DC, 27 (1985).
8. Peebles, L.H., Macromolecules **7**, 872 (1974).
9. Camberlin, Y., Pascault, J.P., J. Polym. Sci. (Polym. Chem. Edn.) **27**, 415 (1983).
10. Lee, H.S., Wang, Y.W., Hsu, S.L., Macromolecules **20**, 2089 (1987).
11. Ryan, A.J., Stanford, J.L., Still, R.H., Brit. Polym. J. **20**, 77 (1988).
12. Davies, W.E., J. Phys. D. Appl. Phys. **4**, 1176 (1971).
13. Kerner, E.H., Proc. Phys. Soc. London **69B**, 808 (1956).

Accepted November 15, 1989 C